

# Application of bio-cementation for loess-slope surface erosion mitigation

Xiaohao SUN<sup>1</sup>, Linchang MIAO<sup>1</sup>, and Runfa chen<sup>1</sup>

<sup>1</sup>Southeast University

May 5, 2020

## Abstract

Bio-cementation, or microbially induced calcite precipitation (MICP), has been shown to mitigate sand erosion; however, only few studies have used it on loess. This study used MICP to investigate the effects of this technology on the improvement of the surface erosion resistance of a loess-slope. Polyvinyl acetate (PVAc) was added to the cementation solution to further increase slope stability. The obtained results showed that MICP treatment resulted in an improvement of erosion resistance and treatment with 6 L/m<sup>2</sup> of mixed solution achieved the best erosion control and highest surface strength. However, the loss of soil in MICP treated slopes still remained large. After adding PVAc to the cementation solution, the stability of the loess-slope increased significantly and resulted in less soil loss and increased surface strength. With 60 g/L PVAc, the surface strength of the slope decreased compared with 40 g/L PVAc because of the thinner depth of cementation. The high erosion resistance of the slope with added PVAc could be attributed to (1) the stable spatial structure of precipitation, and (2) the stronger resistance to tension or shear force from PVAc. These results demonstrated that MICP-PVAc treatment significantly mitigated surface erosion of loess-slopes, which presents promising potential for application in the field.

## Introduction

Loess is a type of globally distributed aeolian silt (Smalley, 1995). In China, the loess area is about 630,000 km<sup>2</sup> and the Loess Plateau is an almost continuous area of loess. The Loess Plateau has an area of 440,000 km<sup>2</sup> with a maximum loess thickness of > 300 m (Liu, 1985; Derbyshire, 2001). However, several particular characteristics of this loess frequently cause geological disasters on the loess slopes of the Loess Plateau, such as soil erosion and landslides (Hu et al., 2018; Xu et al., 2019). Previous studies showed that the total area of soil erosion on the Loess Plateau can reach 340,000 km<sup>2</sup> (Gao et al., 2016; Wu et al., 2018).

Chinese loess is a special geological material that is very sensitive to water erosion and its strength decreases rapidly in response to wetting (Peng et al., 2014; Juang et al., 2019; Derbyshire et al., 2000; Derbyshire, 2001; Xu et al., 2014). In addition, both the shear strength and friction resistance of this loess change with the wetting of the material (Derbyshire et al., 2000; Peng et al., 2017d). Therefore, exposure to rainfall and irrigation damages loess slopes (Zhuang et al., 2017; Leng et al., 2018; Qi et al., 2018; Luo et al., 2018). To better understand the mechanism of landslides and to increase slope stability, a number of engineering interventions and ecological control mechanisms have been studied. Meng et al., (1991) combined shear piles with retaining structures and stabilized and controlled loess landslides in Tianshui, Gansu, China. Jia (2016) summarized the design of retaining walls and Chen et al., (2017) developed a method with which to evaluate the stability of loess slopes that have been affected by water infiltration.

Recently, several traditional treatment methods (e.g., anti-slide piles, anchors, and retaining walls) have been widely used in loess slope engineering to alleviate soil slope instability; however, the negative impact on the surrounding environment is significant and thus, requires attention (Xu et al., 2019). Except for these traditional engineering methods, ecological intervention has also been used to improve the erosion resistance of loess slopes (Wang et al., 2003). However, related ecological intervention techniques may only be suitable for relatively small slopes (Juang et al., 2019). The application potential of afforestation in the semi-arid environment of the Chinese Loess Plateau requires further research. Moreover, the irrigation water required to maintain the afforestation process will also adversely affect the stability of the affected loess slopes.

Bio-cementation or microbially induced calcite precipitation (MICP) is a novel technique in the field of geotechnical engineering. Urea hydrolysis, the most popular MICP pathway, has been widely studied in civil engineering and geological engineering over the past decade. Its essence is the decomposition of urea by bacteria into ammonium ( $\text{NH}_4^+$ ) and carbonate ions ( $\text{CO}_3^{2-}$ );  $\text{CO}_3^{2-}$  can bond with  $\text{Ca}^{2+}$  to achieve carbonate precipitation (e.g., calcium carbonate ( $\text{CaCO}_3$ )) (Sun et al., 2019a, 2019b). With regard to slope erosion mitigation, MICP has been reported to have promising engineering potential to increase both erosion resistance and scour resistance for sand soils (Amin et al. 2017; Gao et al. 2019; Jiang and Soga 2017; Wang et al. 2018). Jiang et al., (2019) studied the feasibility of MICP as a method to control erosion on sandy slopes by using a  $30^\circ$  artificial slope model. In addition to slope erosion, MICP can also effectively improve the coastal sand erosion resistance by simulating tidal cycles (Shanahan and Montoya 2014; Khan et al. 2015; Salifu et al. 2016). However, few reports investigated the use of MICP to mitigate loess-slope surface erosion.

This study used MICP as a loess-slope erosion mitigation method and evaluated the treatment effect through laboratory experiments. Several model loess-slopes were prepared, and in reference to Jiang et al., (2019), bacterial suspensions and cementation solutions were sprayed to part of these artificial loess-slopes. Since soil erosion on the Loess Plateau is mainly caused by rainfall (Zhang and Zhu 2006; Wu et al., 2016a; Wang et al., 2006), rainfall was simulated and the characteristics of the eroded surface and the weight of lost soils were assessed to evaluate the treatment effect. However, several previous field and laboratory tests have shown that water can penetrate deep into thick loess through microporous networks, which results in loss of strength (Derbyshire et al., 2000; Zhuang et al., 2017; Peng et al., 2017d). Thus, if only MICP is used, the loess slope might still collapse because of water flow. As a consequence, Polyvinyl acetate (PVAc) emulsion was used to maintain the stability of the loess surface structure, so that  $\text{CaCO}_3$  produced via MICP could fill the pores of the microporous networks and thus cement loess particles. Similarly, MICP-treated and MICP-PVAc-treated slope models were compared to demonstrate the improvement after PVAc addition.

## Materials and Methods

### *Bacteria and culture medium*

This study used the ureolytic bacterium *Sporosarcina pasteurii* (ATCC 11859, from the Guangdong culture collection centre of China), was used. The culture medium contained yeast extract 20.0 g/L, polypeptone 10.0 g/L,  $(\text{NH}_4)_2\text{SO}_4$  4 g/L, NaCl 8.0 g/L, and distilled water. *S. pasteurii* was grown in the medium. The medium was prepared with deionized water and was autoclaved at  $121^\circ\text{C}$  for 20 min. The initial pH of the medium was 7.0 and the urea concentration was 20 g/L. Media and inoculants were placed on a shaker table at  $30^\circ\text{C}$  for 48 h of growth.

Previous research indicated that absorbance and urease activity were often used to represent the growth characteristic and urealysis ability of bacteria (Sun et al., 2018a; Sun et al., 2018b; Stocks-Fischer et al., 1999). Changes in cell density were assessed by monitoring the absorbance (optical density (OD)) of the suspension at a wavelength of 600 nm ( $OD_{600}$ ) (Fredrickson et al., 2001). The urease activity

was measured as the rate of conductivity increase because of the very strong positive linkage between the increase of conductivity and urea hydrolysis (Chin and Kroontje, 1962; Omoregie et al., 2017). A bacterial suspension with OD<sub>600</sub> of 1.205 and urease activity of 0.712 mM urea hydrolysed/min was used for all subsequent tests.

## *Loess*

Loess from the Loess hilly area of Ningxia province in China was used for all tests. The specific gravity of collapsible loess was 2.721. To obtain the gradation of loess, particle analysis tests were performed. The particle size distribution curve is shown in **Fig. 1**. The collapsible loess was mainly medium silty soil and coarse silty soil, with a clay content of about 20%. The plastic limit was 21.48%, the liquid limit was 31.34%, and the plasticity index was 9.86. The loess used here contained calcite (CaCO<sub>3</sub>), dolomite (CaMg(CO<sub>3</sub>)<sub>2</sub>), Sodium chloride (NaCl), magnesium sulfate (MgSO<sub>4</sub>), calcium sulfate (CaSO<sub>4</sub>), and other ions.

## *Experimental setup*

The tests to determine loess slope erosion and the application of treatment solutions were all conducted in a cube-shaped container (0.18 m × 0.24 m × 0.04 m), which consisted of polymethyl methacrylate. The slope angle was fixed at 30° and a collection vessel was used to collect the lost soil after rainfall simulation. A schematic view of the setup is shown in **Fig. 2**. Over the course of the tests, pictures were taken by a digital camera to observe the surface erosion pattern of the loess slopes at 1, 2, 3, 5, 7, 10, 15, 20, 30, 40, and 50 min. All model slopes were prepared under identical conditions so that the testing results were comparable; therefore, the boundary effect was ignored in the tests. During rainfall simulation, the rainfall intensity was 3 mm/min (180 mm/h) and the pH of the utilized water was about 7.8. During tests, the water was sprayed uniformly by a sprayer head on the loess-slope surface.

## *Treating slope with different methods*

### **Microbially induced carbonate precipitation**

For convenient comparison, the initial dry density of model slopes was identical at 1.52 g/cm<sup>3</sup>. Then, the mixed bacteria solution and cementation solution (0.75 M of Ca(Ac)<sub>2</sub>-urea solution) was uniformly sprayed on the artificial loess-slope surfaces. Several researchers used CaCl<sub>2</sub> for application of MICP (Mahawish et al., 2018; Sun et al., 2019a). Calcium carbonate produced from calcium chloride is mainly calcite, but might also be aragonite with calcium acetate, the bonding effect of which is better than that of calcite (Tittelboom et al., 2010). The amount of bacterial solution used here was less, therefore, calcium acetate was used to increase the bonding effect. Khan et al., (2015) reported that cell densities of bacterial suspension extremely affect the production rates for precipitation. Apart from the OD<sub>600</sub> values, urease activity of bacteria also affects the cementation effect (Sun et al., 2018b). Therefore, bacterial suspensions with similar OD<sub>600</sub> and urease activity were used for treatment.

Six identical model slope samples were prepared and were divided into three groups (A, B, and C) according to different volumes of the mixed solution. Each group had two samples (A1, A2; B1, B2, and C1, C2). For the subsequent application and promotion of practical engineering, the amount of the utilized mixed solution was expressed as the spraying amount per unit area; therefore, the amounts of the mixed solution for A1, B1, and C1 were 2 L/m<sup>2</sup>, 4 L/m<sup>2</sup>, and 6 L/m<sup>2</sup>, respectively. With regard to the control sample in each group, the same amount of distilled water was sprayed instead. Then, the slopes were dried at 25 °C for 6 days before subsequent rainfall simulation tests.

### **Microbially induced carbonate precipitation and Polyvinyl acetate**

To further improve loess slope stability, PVAc (CAS: 9003-20-7) emulsion was added to the cementation solution. PVAc is a synthetic resin, prepared by the polymerization of vinyl acetate (Gordon et al., 2019

). PVAc emulsion is a type of water-based and environmentally friendly adhesive (Zhang et al., 2018), which does not negatively impact the environment. Consequently, PVAc was added for better slope erosion mitigation. The addition of PVAc to cementation solution might affect the bacterial activity or the MICP process. Consequently, the effect of the addition of PVAc on bacterial activity and the production rates of calcium carbonate were investigated. The amounts of PVAc added to the cementation solution were 20 g/L, 40 g/L, and 60 g/L.

According to the calculation method proposed by Whiffin, (2004), 6 ml of bacterial suspension was mixed with 54 ml urea solution (1 mol/L) and the electrical conductivity was measured every 5 min. The average change in conductivity per minute ( $ms/cm \cdot min$ ) was calculated and can be converted to the amount of urease hydrolysis per unit time. Eventually, the rate of hydrolysis of urea per minute ( $mM \text{ urea hydrolysed} \cdot min^{-1}$ ) was obtained by multiplying by the dilution factor of 10, which represented enzyme activity. This method was applied to compare the enzyme activity of the bacterial suspension after addition of PVAc. The total volume of the solution was 60 mL; therefore, the amounts of PVAc were 1.2 g, 2.4 g, and 3.6 g.

To investigate the effect of PVAc addition on the production rates of calcium carbonate, PVAc was added to the cementation solution (a mixture of 0.75 M of urea and 0.75 M of calcium) at various amounts (0 g/L, 20 g/L, 40 g/L, and 60 g/L). In this study, the precipitated calcium carbonate was directly evaluated in transparent polypropylene (PP) tubes at a temperature of 30 °C. 20 mL of bacterial suspension of *S. pasteurii* with an  $OD_{600}$  of 1.205 was mixed with 20 mL of cementation solution. In a sterile environment, 12 groups of samples were used, which were divided into four groups according to the amount of PVAc used. Every group consisted of three parallel samples, all with an original pH of 7.0. The evaluation criterion was the precipitation rate of calcium carbonate, i.e., the ratio of the actually produced amount of calcium carbonate to the theoretically calculated total amount, which was obtained after a 48-h reaction process. The measuring method of the actually produced amount of calcium carbonate has been described in Sun et al. (2018a).

During this process, dried samples were weighed and washed with 0.1 mol/L of HCl several times until air bubbles no longer appeared. The lost dry weight caused by acid leaching was evaluated and was assumed to be the weight of the actually precipitated  $CaCO_3$ . The theoretical total mass of  $CaCO_3$  was evaluated by  $C \times V \times M \times t$ , where C represents the concentration of calcium ions in the cementation solution in mol/L, V represents the solution volume in L, M represents the molar mass of  $CaCO_3$  (100.087 g/mol), and t represents the solidifying time in days.

To compare the curing effect of PVAc addition on loess slopes, various amounts of PVAc were added to cementation solution. Five samples (P1, P2, P3, P4, and P5) were prepared. The amount of mixed solution for samples was 6 L/m<sup>2</sup>. The sample P3, P4, and P5 were treated with MICP, and various amounts of PVAc (20 g/L, 40 g/L, and 60 g/L) were added. P2 was used as MICP control sample and was only treated with MICP. Sample P1 was a blank control sample, which sprayed the same amount of distilled water instead. Similarly, the slopes were dried at 25 °C for 6 days before subsequent rainfall simulation tests.

### *Rainfall Simulation Test*

During the rainfall simulation test, the soil that was washed out from the model loess-slopes was collected by a collection vessel and the weight of the loess within the collection vessel was measured at 1, 2, 3, 5, 7, 10, 15, 20, 30, 40, and 50 min.

### *Surface strength test*

Repeated experiments were conducted with the same samples. These samples had not experienced rainfall erosion test, but surface strength test. A soil penetrometer (type: WISO-750-1, Juchuang company, China) was used to measure the surface strength of samples. This soil penetrometer could directly obtain the penetrated depth and surface strength of the soil via insertion of a probe into the soil (Ulusay and Erguler,

2012; Miao et al., 2019 ). The depth of measuring points for surface strengths were all about 0.02 m. The inserting direction was perpendicular to the soil surface. Six measuring points were randomly chosen to measure surface strengths.

## Test Results and Analysis

### *Slopes treated only with microbially induced carbonate precipitation*

#### *Rainfall erosion observation*

After treatment with MICP, the surface erosion pattern of model slopes differed significantly. The results from the rainfall erosion observation under simulated rainfall at 5, 10, and 20 min are shown in **Fig. 3** . For untreated slopes (A2, B2, and C2), the surface erosion pattern was similar and surface erosion could be clearly observed at 5 min. At the beginning, the loess sample showed a collapsing phenomenon. After 5 min, a great amount of loess soils at the top of the slope was washed into the collection vessel, as shown in **Fig. 3(a)** . As shown in **Fig. 3(b)** , at 10 min, more loess was washed out from slopes. After rainfall for 30 min, the slope was destroyed and only a small amount of loess remained in the container, as shown in **Fig. 3(c)** .

After MICP treatment, the stability of slopes improved and there was no loess collapse. In contrast to untreated slopes, soil at the bottom of the slope (A1), instead of the top of slope, was washed out at 5 min, as shown in **Fig. 3(d)** . The reason of this loess loss might not be surface erosion, but slope collapse. **Fig. 3(e)** shows that at 10 min, the amount of soil loss on the upper slope was still small, but damage began to spread from the bottom of the slope. After 30 min, the slope remained significantly damaged because of the smaller volume of the mixed solution (**Fig. 3(f)** ).

With regard to slope B1, the damage of B1 was smaller and had better integrity at 5 min, as shown in **Fig. 3(g)** . After 10 min, damage spread similarly from the bottom of the slope, but the amount of soil loss on the upper slope was smaller (**Fig. 3(h)** ). In contrast to slope A1, at 30 min, there was still a whole part on the upper of B1, as shown in **Fig. 3(i)** .

Compared with slopes A1 and B1, slope C1 (which was treated by 6 L/m<sup>2</sup> mixed solution) achieved better erosion mitigation. **Fig. 3(j)** shows that a portion of the slope surface at the bottom of the slope was washed away within 5 min. However, after that, less loess soil was washed out from the bottom of the slope. This was because a large amount of the mixed solution remained at the bottom of the slope because of gravity, which cemented the loess particles together and moved the erosion position to the upper part of the sample, as shown in **Fig. 3(k)** . After 30 min of exposure to rainfall, soil loss was much less significant than in the other two MICP cases (**Figs. 3(l)** ).

#### *Soil loss weight and surface strength*

The accumulative soil loss weights were measured, as shown in **Fig. 4** . For untreated slopes A2, B2, and C2, spraying more water would not decrease the amount of soil washed out, indicating that water did not aid erosion mitigation. The percentage of accumulative soil loss weight exceeded 50% during the initial 10 min. After erosion for 50 min, the value even reached 90%. With MICP treatment, the percentage of eroded soil decreased significantly. The rate of the percentage of accumulative soil loss weight decreased with time, eventually leading to less eroded loess. The total percentages of eroded loess in A1, B1, and C1 after 50 min of exposure to rainfall were about 80%, 65%, and 47%, respectively. The curing effect was worse than that reported by **Jiang et al., (2019)** . The reason was that the total volume of the bacterial solution and the cementation solution used was less and the curing time was shorter. The accumulative loess loss weight in C1 was lower than in A1 and B1. The results were consistent with the rainfall simulation test. A better curing effect was contributed to a higher spraying dosage.

Several researchers used unconfined compressive strength (UCS) to evaluate the cementation effect (Qabany et al., 2012; Mortensen et al. 2011; Collins and Sitar 2009 ). However, the depths of slopes used in this study were insufficient to obtain samples for UCS. This was why surface strengths were reported instead of UCS. Ulusay and Erguler, (2012) also used surface strength as a comparative indicator. Fig. 5 shows that in response to spraying more water, the surface strength increased from 156 kPa to 327 kPa. This was because the loess sample contained a portion of clay soil, which would shrink and thus increase strength. After treatment with MICP, the surface strength further increased because of the produced calcium carbonate. The loess-slope C1 had a larger surface strength (442 kPa), which resulted from more calcium carbonate precipitation. According to previous studies, the cementing properties of calcium carbonate precipitation cemented loose sand particles into a strong unit (Sun et al., 2018a; Whiffin et al. 2007 ). This result confirmed that calcium carbonate precipitation can also cement loess particles.

In conclusion, the results confirmed that MICP treatment improves slope stability, mitigate loess-slope surface erosion, and increases surface strength. The soil loss in C1, however, was still significantly higher than the results of previous research (Salifu et al. 2016 ;Jiang et al., 2019 ). Therefore, a better treatment was necessary to effectively and efficiently control loess-slope surface erosion.

### *Slopes treated with microbially induced carbonate precipitation and Polyvinyl acetate*

#### *Effect of Polyvinyl acetate addition on bacterial urease activity and calcium carbonate production rates*

To investigate the effect of PVAc addition on bacterial urease activity, various concentrations of PVAc were added to urea solution. After adding PVAc, the urease activity only experienced a slight fluctuation, as shown in Fig. 6(a) . Therefore, adding PVAc had little impact on urease activity. The curing effect was significantly affected by the amount of calcium carbonate produced. It was necessary to study the effect of PVAc addition on the production rates of calcium carbonate. Fig. 6(b) shows that with increasing PVAc concentration, the production rates for calcium carbonate increased slightly, from 62% to 67%, and then decreased to 65% again at a PVAc addition of 60 g/L. Consequently, there was little influence on production rates for calcium carbonate after adding PVAc.

#### *Rainfall erosion observation*

After combined treatment with MICP and PVAc, the stability of the loess-slope improved significantly. Pictures of these slopes under simulated rainfall at 10, 20, and 50 min are shown in Fig. 7 . Because changes could not be observed within a short time, the time span of observation in Fig. 7 increased compared that use for Fig. 3 .

In contrast to slopes treated with MICP alone, no slope collapse or soil surface erosion were observed at 10 min, which can be seen in Fig. 7(a) , Fig. 7(d) , and Fig. 7(g) . For P3, a crack at the upper slope emerged at 20 min, as shown in Fig. 7(b) . Water entered from the interior of the sample (P3) through cracks and destroyed the stable internal structure of the sample. At 50 min, the slope was destroyed because of the inefficient cementing effect of the surface ( Fig. 7(c) ). Observing the samples after destruction showed that there was a thin hard surface crust. This hard surface crust was primarily composed of CaCO<sub>3</sub> minerals. Jiang et al., (2019) obtained the same conclusion.

With regard to slope P4, Fig. 7(e) shows a smaller crack at 20 min. However, the growth speed of this crack was lower and after 50 min of exposure to rainfall, the crack still remained small due to better cementing effect. The upheaval happened at the bottom of the slope, as shown in Fig. 7(f) . This was because water entered the interior of the sample (P4), causing part of the loess soil to flow down.

The slope P5, which was treated by MICP and 60 g/L PVAc, had a more complete surface compared with the other two slopes (P3 and P4). Fig. 7(h) shows that no crack appeared within 20 min. However, a small

crack appeared on the upper part of the specimen, at 50 min. After 50 min of exposure to rainfall, this upheaval was much smaller than that of slope P4, as shown in **Fig. 7(i)** .

### *Soil loss weight and surface strength*

Accumulative loess loss weights were measured, as shown in **Fig. 8** . For the untreated slope P1 and the MICP treated slope P2, the same results were obtained via repeated experiments, which verified the correctness and repeatability of the experiment. With regard to slopes (P3, P4, and P5), which were treated with both MICP and PVAc, the weights of the lost loess were much lower than those for P1 and P2. During the initial 15 min, the amounts of lost loess were almost zero. After that, a small amount of soil in slope P3 was washed out; however, the accumulative loess loss weights of slopes P4 and P5 still remained zero because of their better cementing effect. Slope P3 showed a large loess loss from 40 min to 50 min. The eventual accumulative loess loss weights of P4 and P5 after 50 min of exposure to rainfall were only 3.04 and 0 g, respectively. The results were consistent with the rainfall simulation test. The better curing effect of P4 and P5 was contributed to the higher concentration of PVAc. The results confirmed that MICP-PVAc treatment further improved slope stability and mitigated loess-slope surface erosion.

**Fig. 9** shows that with PVAc addition, the surface strength increased from 434 kPa to 486 kPa. This was because of the additional cementing effect of PVAc, as shown in **Fig. 10** , which further increased strength. The loess-slope P4 had a higher surface strength (657 kPa), as a result of the higher concentration of PVAc used. However, with adding PVAc of 60 g/L, the surface strength of slope P5 decreased more than that of slope P4, while still remaining higher than that of slope P3. This suggests that the thickness of cementation of P5 was smaller, while the depth of measuring points for surface strengths were all about 0.02 m, resulting in lower surface strength. The reason is further analysed in the “Thickness of cemented layer” section.

### *Thickness of cemented layer*

After the rainfall simulation test, to obtain the thickness of the cemented layer via calliper, several random measuring points were chosen and sampled perpendicular to the slope surface. The average thickness of the cemented layer was used as indicator to evaluate the achieved cementing effect.

The average values are detailed in **Table 1** . For P2, the thickness of the cemented layer was 24.0 mm, which resulted from MICP treatment. For P3, P4, and P5, the thicknesses of the cemented layer averaged 17.4 mm, 10.6 mm, and 9.3 mm, respectively. These data were much lower than in P2. Despite the thinner cemented layer, MICP-PVAc treatment allowed for better cementing effect than MICP treatment alone. This was the reason why the relevant samples had better surface erosion resistance than P2. For P3, P4, and P5, it was found that a higher concentration of PVAc in cementation solution resulted in a thinner cemented layer. This was because PVAc addition would clog near-surface soil pores. With higher concentration of PVAc in the cementation solution, the mixed solution would be harder to percolate into deeper soil. Furthermore, even if the cemented layer thicknesses of P4 and P5 were less than those of P2 and P3, their erosion resistance was significantly better, as shown in **Fig. 7** and **Fig. 8** . The high erosion resistances of P4 and P5 were attributed to (1) the stable spatial structure of  $\text{CaCO}_3$  precipitation, and (2) the stronger resistance to tension or shear force from PVAc. Both hypotheses will be further analysed in the “Discussion” section.

### *Scanning electron microscope test*

After rainfall simulation test, surface soil samples P2 and P5 were subjected to scanning electron microscope (SEM) test, as shown in **Fig. 11**. **Fig. 11(a)** shows that in response to MICP treatment, a large number of  $\text{CaCO}_3$  crystals were produced between loess particles. In addition to their bridge function,  $\text{CaCO}_3$  crystals were also deposited on the surface of loess particles. Compared with P2, in P5 with MICP-PVAc treatment, several loess particles were coated by PVAc and  $\text{CaCO}_3$  crystals together, which formed a layer-like film. Moreover, the PVAc and  $\text{CaCO}_3$  crystals also contacted loess particles, as shown in **Fig. 11(b)** .

Furthermore, in response to MICP treatment, most  $\text{CaCO}_3$  crystals were spherical with a size of about 3-5

$\mu\text{m}$ , as shown in **Fig. 11(c)**. In addition to spherical crystals, few amorphous crystals were found. However, in contrast to P2, most  $\text{CaCO}_3$  crystals in **Fig. 11(d)** were amorphous crystals. The size of  $\text{CaCO}_3$  crystals remained below  $1 \mu\text{m}$ , and these small crystals were clumped together.

## Discussion

### *Treatment of microbially induced calcite precipitation and Polyvinyl acetate together*

The PVAc emulsion is mainly composed of a vinyl acetate (VAc) monomer. VAc can be copolymerized with various monomers, including acrylate, ethylene, vinyl chloride, Veova 10, and methyl methacrylate monomers (Dossi et al., 2010; Sarac and Yildirim, 2006; Rosdi and Ariffin, 2016; Ahmed et al., 2017). Such adhesives are used for bonding of wood, paper, and fabric. If PVAc was used for slope treatment, the volume would be large, resulting in higher costs. PVAc emulsions have satisfactory gap-filling properties (Shields 1984). Therefore, PVAc and MICP can be used together to bond particles and form a more stable structure, as shown in **Fig. 10**. With low PVAc concentration, the microstructure forms a network structure (Jaziet al., 2019). This decreases the cost by decreasing the required PVAc concentration. In addition, the network structure of PVAc is beneficial to affix the calcium carbonate, which might be a common characteristic for this type of high-molecular polymer. Miao et al., (2019) also reported that Polyacrylamide had the same effect. The structure was confirmed by SEM tests.

During exposure to rainfall, particles are subject to tension and shear forces, which determines the erosion resistance. De Jong et al., (2006) showed that for samples treated with MICP, most of the failure interface was inside calcium carbonate, i.e., the generated calcium carbonate was fractured inside after failure. Therefore, it was necessary to increase the resistance to tension and shear forces. By adding PVAc at low concentration, the network structure can provide stronger resistance to tension or shear force, thus avoiding calcium carbonate fracture inside and improving the slope stability.

### *Scanning electron microscope test*

SEM testing can be used to compare the difference among specimen from a microscopic perspective (Delage et al. 2006). After rainfall simulation test, surface soil samples P2 and P5 were subjected to SEM test, as shown in **Fig. 11**. Compared with P2 (MICP treatment), in P5 with MICP-PVAc treatment, several loess particles were coated by PVAc and  $\text{CaCO}_3$  crystals together, resembling a film. Moreover, between loess particles, PVAc formed a net structure, which provides bonding force and tension force, as shown in **Fig. 11(b)**.

Furthermore, in contrast to P2, most  $\text{CaCO}_3$  crystals in **Fig. 11(d)** were amorphous crystals, which were held in place by PVAc. The  $\text{CaCO}_3$  crystals were small and clumped together. The reason was that the growth of  $\text{CaCO}_3$  crystals was affected by PVAc, so that the crystals could not grow into a large sphere, but rather, grew into a group of amorphous crystals. In conclusion, the SEM photos showed that the more stable spatial net structure in P5 was confirmed.

## Conclusions

Bio-cementation tests were conducted to investigate the effects of the combined MICP-PVAc technology on the improvement of loess-slope surface erosion resistance. Moreover, PVAc was added to the cementation solution, which further improved slope stability. The results demonstrated that MICP-PVAc treatment significantly mitigated surface erosion of loess-slope. Specific conclusions are outlined as follows:

(1) MICP treatment resulted in an improvement of erosion resistance and treatment with  $6 \text{ L/m}^2$  of mixed solution achieved the best erosion control and the highest surface strength. The soil loss in MICP treated

slopes, however, still remained large. Therefore, a better treatment was necessary to effectively and efficiently control the erosion of loess-slope surfaces.

(2) Addition of PVAc had little impact on urease activity and production rates for calcium carbonate. After treatment with MICP and PVAc together, the stability of loess-slope improved significantly. For slopes treated with the addition of PVAc at 40 g/L or 60 g/L, 50 min of exposure to rainfall caused little soil loss because of the better cementing effect.

(3) With the addition of PVAc to the cementation solution, the surface strength of slopes increased beyond that of slopes treated with MICP only. With 60 g/L PVAc, the surface strength of slope P5 decreased below that of slope P4, but still remained higher than that of slope P3 because of the lower thickness of cementation.

(4) The high erosion resistance of P4 and P5 was attributed to (1) the stable spatial structure of  $\text{CaCO}_3$  precipitation, and (2) the stronger resistance to tension or shear force from PVAc. The method proposed in this study provides an effective and efficient technique for loess-slope erosion control, with promising potential for application in the field.

### **Data Availability Statement**

No data, models, or code were generated or used during the study.

### **Acknowledgments**

The design idea of the experimental device in this paper comes from Jiang et al., (2019), for which the authors would like to express our thanks. The authors thank the valuable comments from the reviewers.

### **Compliance with Ethical Standards**

Funding:

This study was funded by National Natural Science Foundation of China (grant number 51578147).

Conflict of Interest:

Author1 declares that he has no conflict of interest.

Author2 declares that he has no conflict of interest.

Author3 declares that he has no conflict of interest.

Ethical approval:

“This article does not contain any studies with human participants performed by any of the authors.”

### **References**

- Ahmed, M.; Abd-Elhamid, M.; Sarhan, A.; Hassan, A. Characteristic and thermal stimulated depolarization current of poly (vinyl chloride-co-vinyl acetate-co-2-hydroxy propyl acrylate) Znnonanocomposite. *Glob. J. Phys.* 2017, 5, 585–594.
- Amin, M., S. M. A. Zomorodian, and B. C. O’Kelly. 2017. “Reducing the hydraulic erosion of sand using microbial-induced carbonate precipitation.” *Proc. Inst. Civ. Eng. Ground Improv.* 170 (2): 112–122.
- Chen, H.J., Han, Z.F., Zhou, C.M., Zhang, X.W., 2017. Stability analysis of high slope in loess cut under rainfall. *Highway* 2, 6–11 (in Chinese).
- Chin W T, Kroontje W (1962) Conductivity Method for Estimation of Enzyme activity. *Agricultural and Food Chemistry*, 10: 347-348
- Collins, B.D., Sitar, N., 2009. Geotechnical properties of cemented sands in steep slopes. *J. Geotech. Geoenviron. Eng.* 135 (10), 1359–1366

Dejong J T, Fritzes M B, Nüsslein K. Microbially induced cementation to control sand response to undrained shear. *Journal of Geotechnical and Geoenvironmental Engineering*, 2006, 132(11): 1381-1392.

Delage, P., D. Marcial, Y. J. Cui, and X. Ruiz. 2006. "Ageing effects in a compacted bentonite: A microstructure approach." *Géotechnique* 56 (5): 291–304. <https://doi.org/10.1680/geot.2006.56.5.291>.

Derbyshire, E., 2001. Geological hazards in loess terrain, with particular reference to the loess regions of China. *Earth-Sci. Rev.* 54 (1–3), 231–260.

Derbyshire, E., Meng, X.M., Dijkstra, T., 2000. Landslides in the Thick Loess Terrain of North-West China. John Wiley and Sons Ltd, London.

Dijkstra, T.A., Smalley, I.J., Rogers, C.D.F., 1995. Particle packing in loess deposits and the problem of structure collapse and hydroconsolidation. *Eng. Geol.* 40 (1–2), 49–64.

Dossi, M.; Liang, K.; Hutchinson, R.A.; Moscatelli, D. Investigation of free-radical copolymerization propagation kinetics of vinyl acetate and methyl methacrylate. *J. Phys. Chem. B* 2010, 114, 4213–4222.

Fredrickson J K, Fletcher M, Frederickson J K, et al. Subsurface microbiology and biogeochemistry[J]. John Wiley & Sons, 2001.

Gao, G.R., 1988. Formation and development of the structure of collapsing loess in China. *Eng. Geol.* 25 (2), 235–245

Gao HD, Li ZB, Jia LL, Li P, Xu GC, Ren ZP, Pang GW (2016) Capacity of soil loss control in the loess plateau based on soil erosion control degree. *J Geogr Sci* 26(4):457–472.

Gao, Y., X. Tang, J. Chu, and J. He. 2019. "Microbially induced calcite precipitation for seepage control in sandy soil." *Geomicrobiol. J.* 36 (4): 366–375.

Gordon P. Bierwagen J. Preston Malcolm P. Stevens Ferdinand Rodriguez George B. Kauffman Alan N. Gent. 2019. Major industrial polymers. *Encyclopædia Britannica*, inc.

Hu S, Jiao J, Garcia-Fayos P, Kou M, Chen Y, Wang W. 2018. Telling a different story: plant recolonization after landslides under a semi-arid climate. *Plant Soil.* 426(1–2):163.

Jazi, M. A., SA, A. R., Haddadi, S. A., Ghaderi, S., & Azamian, F. (2019). In situ emulsion polymerization and characterization of PVAc nanocomposites including colloidal silica nanoparticles for wood specimens bonding. *Journal of Applied Polymer Science*.

Jia, Y.J., 2016. Research on concrete retaining wall reinforced unsaturated loess slope. *China Build. Mater. Sci. Technol* 25 (4), 107–108 (in Chinese).

Jiang, N.-J., and K. Soga. 2017. "The applicability of microbially induced carbonate precipitation for internal erosion control in gravel-sand mixtures." *Géotechnique* 67 (1): 42–55.

Jiang, N. J., Tang, C. S., Yin, L. Y., Xie, Y. H., & Shi, B. (2019). Applicability of microbial calcification method for sandy-slope surface erosion control. *Journal of Materials in Civil Engineering*, 31(11), 04019250.

Juang, C. H., Dijkstra, T., Wasowski, J., & Meng, X. (2019). Loess geohazards research in China: Advances and challenges for mega engineering projects. *Engineering geology*, 251, 1-10.

Khan, M. N. H., G. G. N. N. Amarakoon, S. Shimazaki, and S. Kawasaki. 2015. "Coral sand solidification test based on microbially induced carbonate precipitation using ureolytic bacteria." *Mater. Trans.* 56 (10): 1725–1732.

Leng, Y., Peng, J., Wang, Q., Meng, Z., Huang, W., 2018. A fluidized landslide occurred in the Loess Plateau: a study on loess landslide in South Jingyang Tableland. *Eng. Geol.* 236, 129–136.

Liu, T.S., 1985. *Loess and the Environment*. Science Press, Beijing (in Chinese).

- Luo, H., Wu, F.Q., Chang, J.Y., Xu, J.B., 2018. Microstructural constraints on geotechnical properties of Malan Loess: a case study from Zhaojiaan landslide in Shaanxi province, China. *Eng. Geol.* 236, 60–69.
- Mahawish, A., Bouazza, A., Gates, W. P. (2018). Effect of particle size distribution on the bio-cementation of coarse aggregates. *Acta Geotechnica*, 13(4), 1019-1025.
- Meng, X.M., Xu, Y.H., Guo, T., Zhang, S.W., 1991. Research of Jiaoshuwan and Taishanmiao landslides in Tianshui city. *J. Gansu Sci* 3 (2), 36–43 (in Chinese).
- Miao, L., Wu, L., Sun, X., Li, X., Zhang, J. 2019. Method of Solidifying Desert Sands with Enzyme-Catalysed Mineralization. *Land Degradation & Development*.
- Mortensen, B. M., M. J. Haber, J. T. DeJong, L. F. Caslake, and D. C. Nelson. 2011. “Effects of environmental factors on microbial induced calcium carbonate precipitation.” *J. Appl. Microbiol.* 111 (2): 338–349.
- Omoriegic A I, Khoshdelnezamiha G, Senian N, et al. (2017) Experimental optimisation of various cultural conditions on urease activity for isolated sporosarcina pasteurii strains and evaluation of their biocement potentials. *Ecol. Eng.*, 109, 65–75.
- Peng, J.B., Lin, H.Z., Wang, Q.Y., Zhuang, J.Q., Cheng, Y.X., Zhu, X.H., 2014. The critical issues and creative concepts in mitigation research of loess geological hazards. *J. Eng. Geol.* 22 (4), 684–691 (in Chinese)
- Peng, J.B., Wang, G.H., Wang, Q.Y., Zhang, F.Y., 2017d. Shear wave velocity imaging of landslide debris deposited on an erodible bed and possible movement mechanism for a loess landslide in Jingyang, Xi’an, China. *Landslides* 14, 1503–1512.
- Qabany, A. A., K. Soga, and C. Santamarina 2012. “Factors affecting efficiency of microbially induced calcite precipitation.” *J. Geotech. Geoenviron. Eng.* 138 (8): 992–1001.
- Qi, X., Xu, Q., Liu, F.Z., 2018. Analysis of retrogressive loess flow slides in Heifangtai, China. *Eng. Geol.* 236, 119–128.
- Rosdi, M.R.H.; Ariffin, A. Evaluation of flow ability response in EVA emulsion preparation with different vinyl acetate percentage by intrinsic viscosity measurement. *Procedia Chem.* 2016, 19, 455–461.
- Salifu, E., E. MacLachlan, K. R. Iyer, C. W. Knapp, and A. Tarantino. 2016. “Application of microbially induced calcite precipitation in erosion mitigation and stabilisation of sandy soil foreshore slopes: A preliminary investigation.” *Eng. Geol.* 201 (Feb): 96–105.
- Sarac, A.; Yildirim, H. Semi-continuous emulsion copolymerization of vinyl acetate and butyl acrylate using a new protective colloid. Part 1. Effect of different emulsifiers. *Polym. Adv. Technol.* 2006, 17, 855–859.
- Shanahan, C., and B. M. Montoya. 2014. “Strengthening coastal sand dunes using microbial-induced calcite precipitation.” In *Proc. GeoCongress 2014, GSP 234*, edited by M. Abu-Farsakh, X. Yu, and L. R. Hoyos. Reston, VA: ASCE.
- Shields J. *Adhesives handbook*. 3rd ed. London: Butterworths Heinemann; 1984.
- Smalley, I., 1995. Making the material: the formation of silt sized primary mineral particles for loess deposits. *Quat. Sci. Rev.* 14 (7–8), 645–651.
- Stocks-Fischer, S., Galinat, J. K., Bang, S. S. Microbiological precipitation of CaCO<sub>3</sub>. *Soil Biology and Biochemistry*, 1999, 31(11), 1563-1571.
- Sun X H, Miao L C, Tong T Z, et al. (2018a) Improvement of Microbial-Induced Calcium Carbonate Precipitation Technology for Sand Solidification. *J. Mater. Civ. Eng.*, 30(11), 04018301.

- Sun X H, Miao L C, Tong T Z, et al. (2018b) Study of the effect of temperature on microbially induced carbonate precipitation. *Acta Geotech.*, 14(3), 627-638.
- Sun, X., Miao, L., Chen, R. (2019a). Effects of Different Clay's Percentages on Improvement of Sand-Clay Mixtures with Microbially Induced Calcite Precipitation. *Geomicrobiology Journal*, 1-9.
- Sun, X., Miao, L., Wu, L., & Chen, R. (2019b). Improvement of bio-cementation at low temperature based on *Bacillus megaterium*. *Applied microbiology and biotechnology*, 103(17), 7191-7202. <https://doi.org/10.1007/s00253-019-09986-7>.
- Tittelboom K V, Belie N D, Muynck W D, et al., 2010. Use of bacteria to repair cracks in concrete. *Cement & Concrete Research*, 40(1):157-166.
- Ulusay, R., & Erguler, Z. A. Needle penetration test: evaluation of its performance and possible uses in predicting strength of weak and soft rocks. *Engineering geology*, 2012, 149, 47-56. <https://doi.org/10.1016/j.enggeo.2012.08.007>.
- Wang B, Steiner J, Zheng F, Gowda P (2017) Impact of rainfall pattern on interrill erosion process. *Earth Surf Process Landf* 42(12):1833–1846.
- Wang, G.A., Han, J.M., Liu, D.S., 2003. The carbon isotope composition of C3 herbaceous plants in loess area of northern China. *Sci. China* 46 (10), 1069–1076.
- Wang H, Wang QJ, Shao MA (2006) Laboratory experiments of soil nutrient transfer in the loess slope with surface runoff during simulated rainfall. *Trans Chin Soc Agric Eng* 22(6):39–44
- Wang, X., J. Tao, R. Bao, T. Tran, and S. Tucker-Kulesza. 2018. "Surficial soil stabilization against water-induced erosion using polymermodified microbially induced carbonate precipitation." *J. Mater. Civ. Eng.* 30 (10): 04018267.
- Whiffin V S (2004) Microbial CaCO<sub>3</sub> precipitation for the production of biocement. Perth, Australia: Murdoch University.
- Whiffin V S, van Paassen L A, Harkes M P. Microbial carbonate precipitation as a soil improvement technique. *Geomicrobiology Journal*, 2007, 24(5): 417-423.
- Wu L, Liu X, Ma XY (2016a) Spatiotemporal distribution of rainfall erosivity in the Yanhe River watershed of hilly and gully region, Chinese Loess Plateau. *Environ Earth Sci* 75(4):315.
- Wu L, Liu X, Ma XY (2016b) Application of a modified distributed dynamic erosion and sediment yield model in a typical watershed of a hilly and gully region, Chinese Loess Plateau. *Solid Earth* 7(6): 1577–1590.
- Wu, L., Peng, M., Qiao, S., & Ma, X. Y. (2018). Effects of rainfall intensity and slope gradient on runoff and sediment yield characteristics of bare loess soil. *Environmental Science and Pollution Research*, 25(4), 3480-3487.
- Xu, L., Dai, F.C., Tu, X.B., Tham, L.G., Zhou, Y.F., Iqbal, J., 2014. Landslides in a Loess Platform, North-West China. *Landslides* 11 (6), 993–1005.
- Xu, R., Li, X., Yang, W., Jiang, C., & Rabiei, M. (2019). Use of local plants for ecological restoration and slope stability: a possible application in Yan'an, Loess Plateau, China. *Geomatics, Natural Hazards and Risk*, 10(1), 2106-2128.
- Zhang, Y., Pang, B., Yang, S., Fang, W., Yang, S., Yuan, T. Q., & Sun, R. C. (2018). Improvement in Wood Bonding Strength of Poly (Vinyl Acetate-Butyl Acrylate) Emulsion by Controlling the Amount of Redox Initiator. *Materials*, 11(1), 89.
- Zhang Y, Zhu QK (2006) Analysis on eroded rainfall characteristics of Loess Plateau. *Res Environ Arid Land* 06:99–103.

**Table 1** Cementation layer thickness of slopes treated with different methods

Sample No.	Average entire cemented layer thickness (mm)	Curing method
P1	/	Untreated
P2	24.0	MICP-treated
P3	17.4	20 g/L PVAc-treated
P4	10.6	40 g/L PVAc-treated
P5	9.3	60 g/L PVAc-treated

**Figure Captions**

**Figure 1.** Particle size distribution of loess materials

**Figure 2.** Schematic set-up of the rainfall simulation test device

**Figure 3.** Visual observation of surface erosion patterns of slopes treated with MICP and subjected to artificial rainfall for indicated durations: (a) A2, 5 min; (b) A2, 10 min; (c) A2, 20 min; (d) A1, 5 min; (e) A1, 10 min; (f) A1, 20 min; (g) B1, 5 min; (h) B1, 10 min; (i) B1, 20 min; (j) C1, 5 min; (k) C1, 10 min; and (l) C1, 20 min

**Figure 4.** Accumulative soil loss weight of slopes treated with MICP

**Figure 5.** Surface strength of slopes treated with MICP

**Figure 6.** Urease activity and production rates of calcium carbonate after PVAc addition: (a) Urease activity;(b) production rates for calcium carbonate

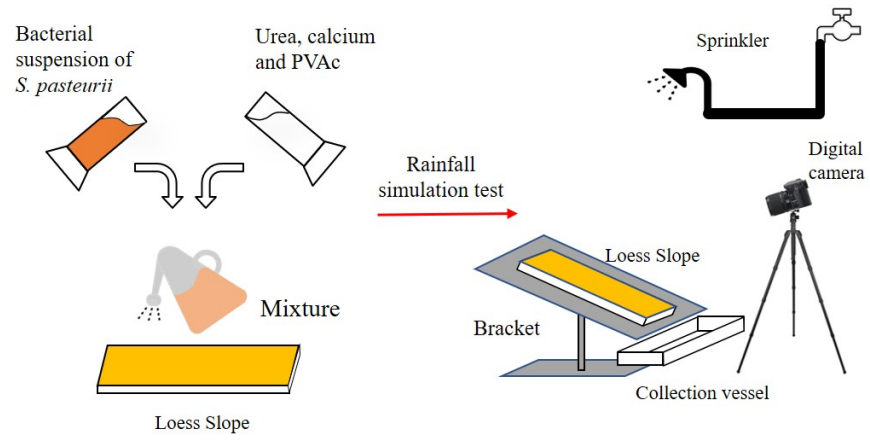
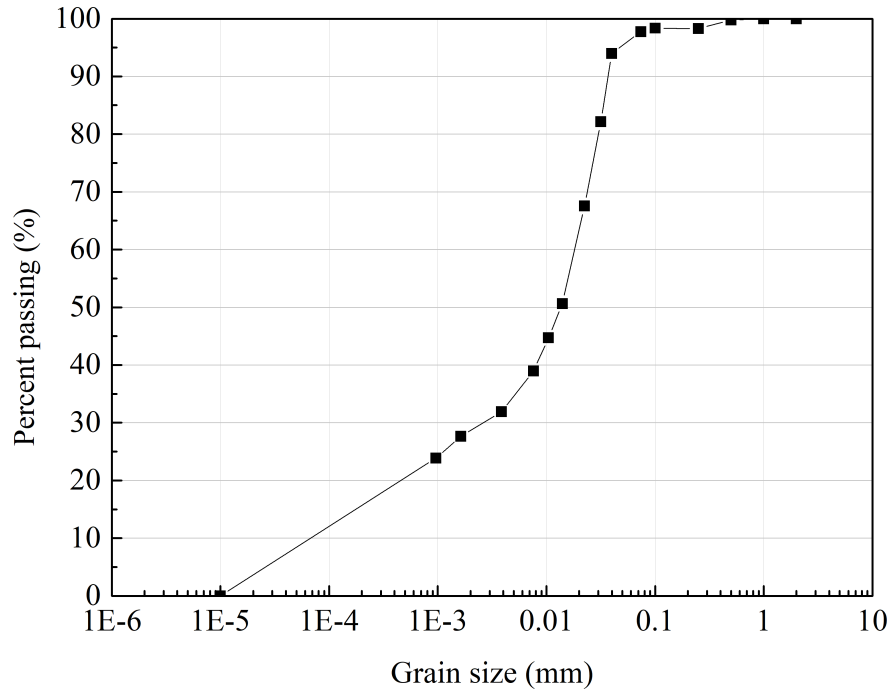
**Figure 7.** Visual observation of surface erosion patterns of slopes treated with MICP and PVAc: (a) P3, 10 min; (b) P3, 20 min; (c) P3, 50 min; (d) P4, 10 min; (e) P4, 20 min; (f) P4, 50 min; (g) P5, 10 min; (h) P5, 20 min; (i) P5, 50 min

**Figure 8.** Accumulative soil loss weight of slopes treated with MICP and PVAc

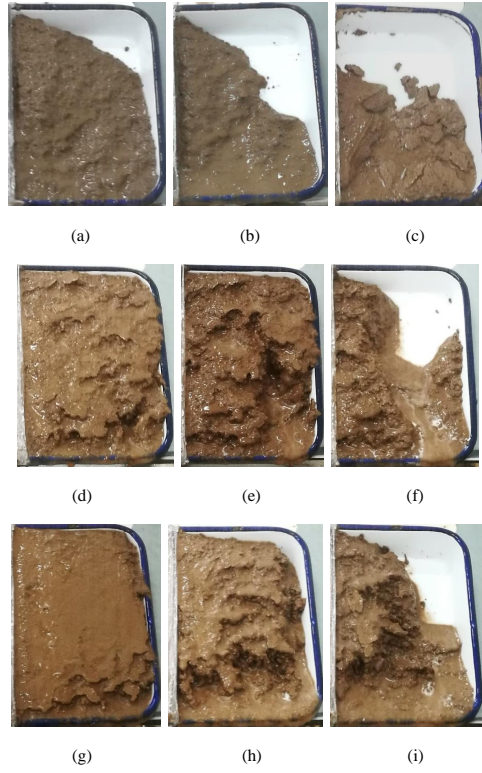
**Figure 9.** Surface strength of slopes treated with MICP and PVAc

**Figure 10.** Schematic diagram of cementation between particles

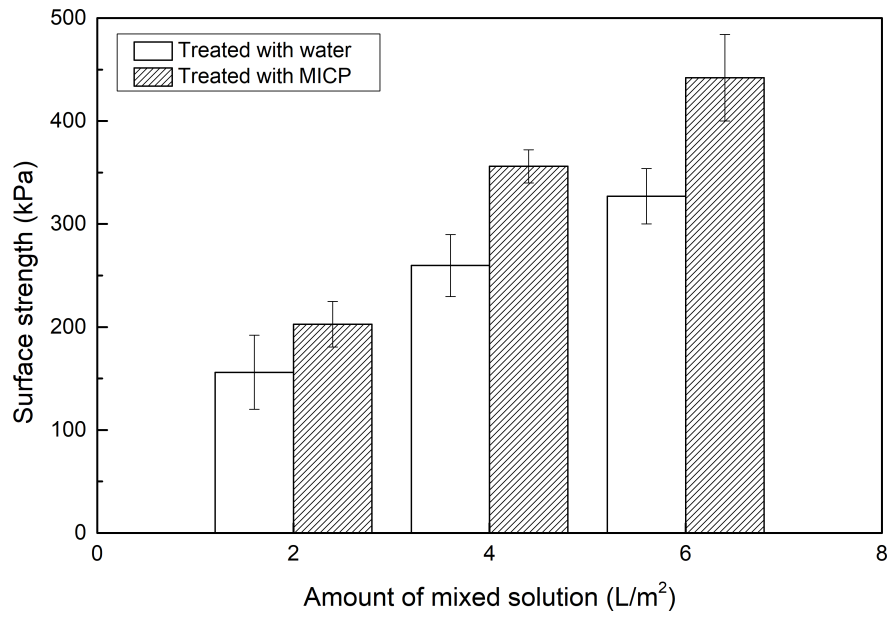
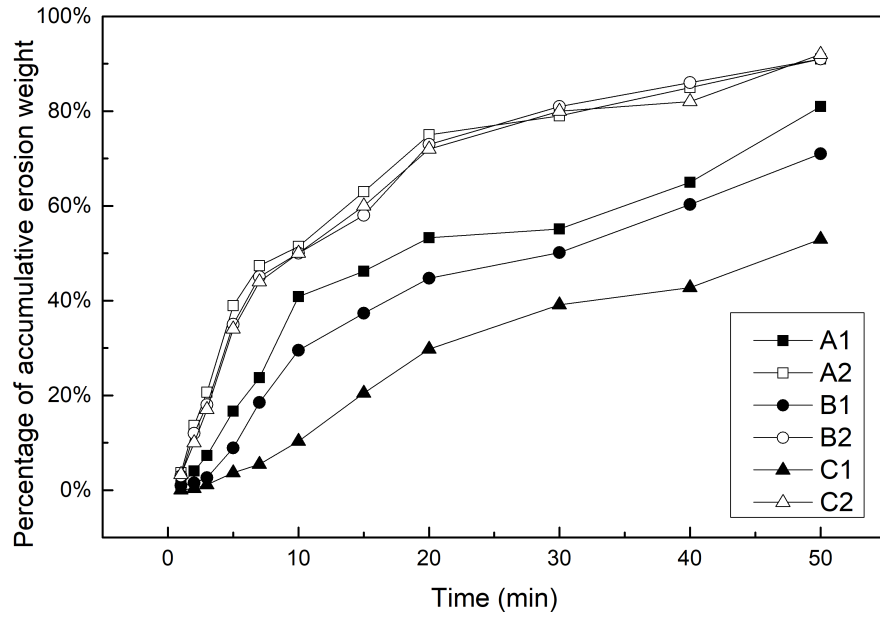
**Figure 11.** SEM images of treated slopes after rainfall simulation tests: (a) P2, magnification = 2500×; (b) P5, magnification = 2500×; (c) P2, magnification = 20000×; (d) P5, magnification = 20000×.

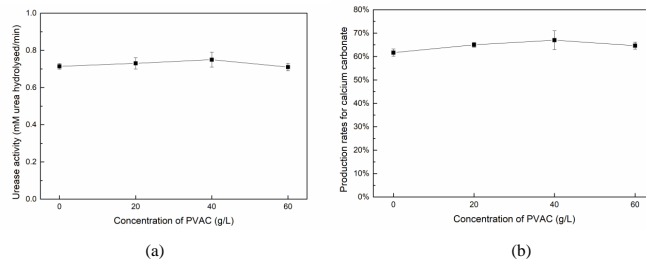


1  
2  
3  
4  
5  
6  
7



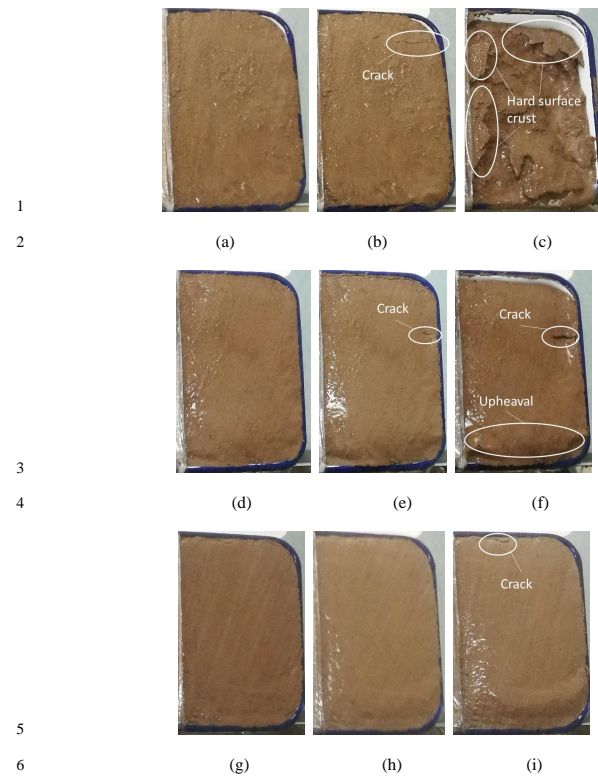
1





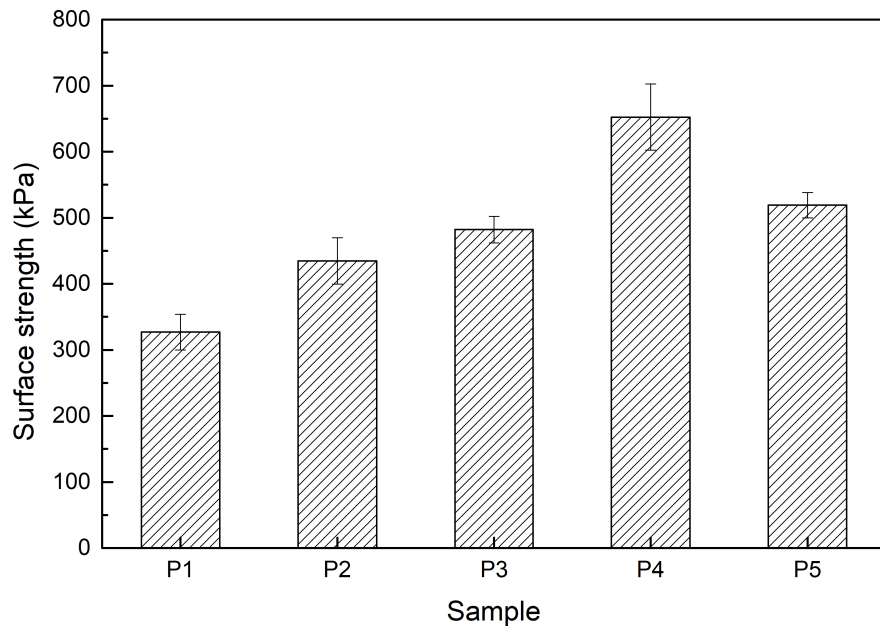
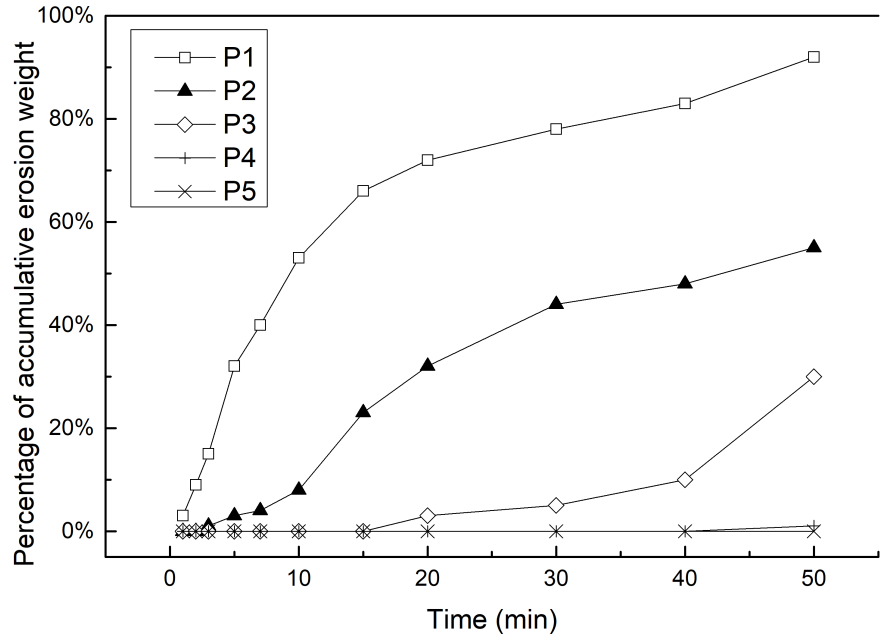
1  
2  
3  
4  
5

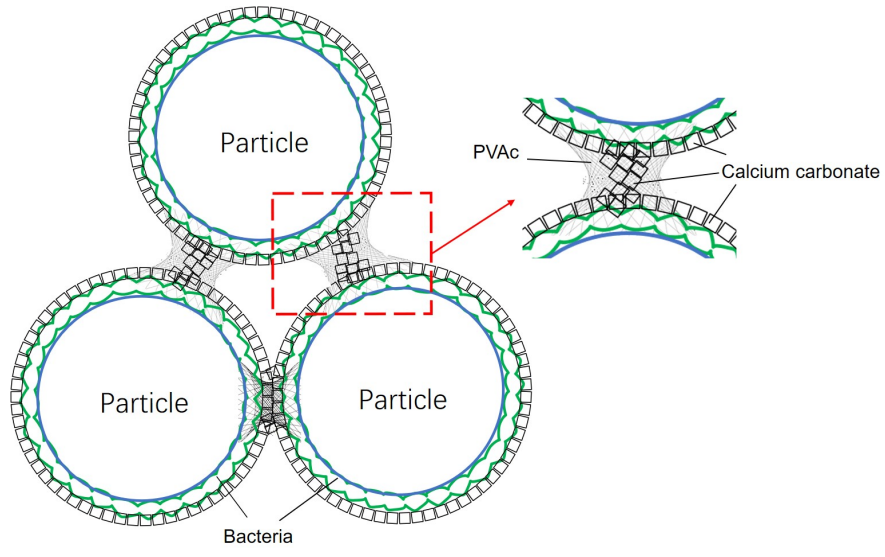
**Figure 6.** Urease activity and Production rates for calcium carbonate after adding PVAc: (a) Urease activity; (b) Production rates for calcium carbonate

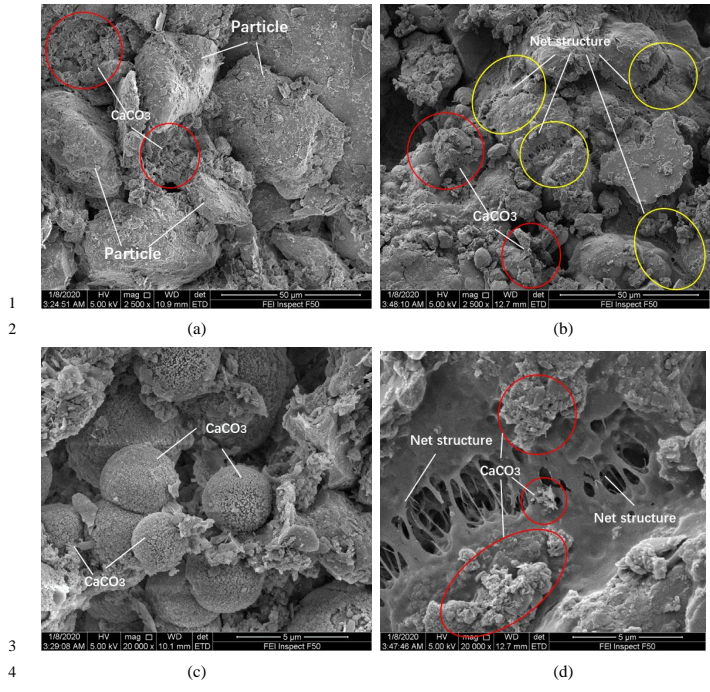


7 **Figure 7.** Visual observation of surface erosion patterns of slopes treated with MICP and PVAc:  
8 (a) P3, 10 min; (b) P3, 20 min; (c) P3, 50 min; (d) P4, 10 min; (e) P4, 20 min; (f) P4, 50 min; (g)  
9 P5, 10 min; (h) P5, 20 min; (i) P5, 50 min

10







1  
2  
3  
4  
5 **Figure 11.** SEM images of the treated slope after rainfall simulation test: (a) P2, magnification  
6 =2500×; (b) P5, magnification=2500×; (c) P2, magnification =20000×; (d) P5, magnification  
7 =20000×.  
8